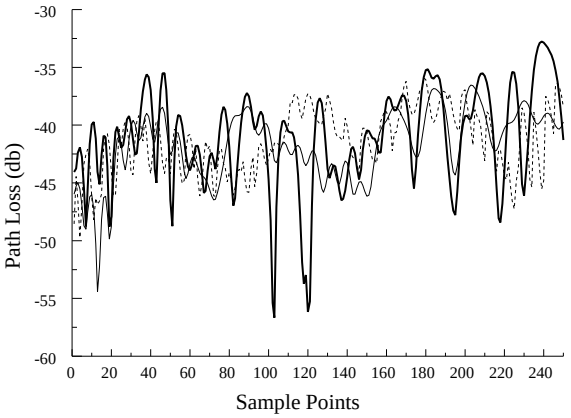

Figure 4 Simulation results. ——— FDTD (periodic), ——— FDTD (uniform), -------- ray tracing (uniform)

ference in the periodic structure using the FDTD method and the ray-tracing method is more than 18 dB.

CONCLUSION

In this letter, we use the FDTD method to see the effect of the inner structure of a wall on indoor propagation prediction. The ray-tracing method cannot deal with nonspecular reflection caused by higher order Floquet modes. A comparison of the FDTD method with the ray-tracing method shows that the FDTD method can give accurate results everywhere in the considered area when the environment is complex, but not too large.

REFERENCES

1. U. Dersch and E. Zolllinger, Propagation mechanism in microcell and indoor environments, IEEE Trans Veh Technol 43 (1994), 1058–1066.
2. R.A. Valenzula, O. Landron, and D.L. Jacobs, Estimating local mean signal strength of indoor multipath propagation, IEEE Trans Veh Technol 46 (1997), 203–212.
3. J.H. Tarng, W.R. Chang, and B.J. Hsu, Three-dimensional modeling of 900-MHz and 2.44-GHz radio propagation in corridors, IEEE Trans Veh Technol 46 (1997), 519–526.
4. W. Honcharenko and H.L. Bertoni, Transmission and reflection characteristics at concrete block walls in the UHF bands proposal for future PCs, IEEE Trans Antennas Propagat 42 (1994), 232–239.
5. C.L. Holloway and P.L. Perini, Analysis of composite walls and their effects on short-path propagation modeling, IEEE Trans Veh Technol 46 (1997), 730–738.

COMBINING FDTD SIMULATIONS WITH MEASUREMENTS OF MICROSTRIP RING RESONATORS FOR CHARACTERIZATION OF LOW- AND HIGH-*K* DIELECTRICS AT MICROWAVES

Elena Semouchkina,[1] Wenwu Cao,[1, 2] Michael Lanagan,[1] Raj Mittra,[3] and Wenhua Yu[3]
[1] Materials Research Laboratory
The Pennsylvania State University
University Park, Pennsylvania 16802
[2] Department of Mathematics
The Pennsylvania State University
University Park, Pennsylvania 16802
[3] Department of Electrical Engineering
The Pennsylvania State University
University Park, Pennsylvania 16802

Received 13 September 2000; revised 8 November 2000

ABSTRACT: *This paper shows how the dielectric constant of alumina and rutile substrates at microwave frequencies can be accurately determined by fitting the simulated S-parameter spectra of microstrip ring resonators, generated via the finite-difference time-domain (FDTD) method, to experimentally measured data. The proposed method does not require the determination of the effective dielectric constant and the approximate closed-form expressions to find the true permittivity of the substrate. This is essential for the characterization of high-K dielectric materials at high frequencies when the closed-form expressions are invalid.* © 2001 John Wiley & Sons, Inc. Microwave Opt Technol Lett 29: 21–24, 2001.

Key words: *finite-difference time-domain method; dielectric characterization; microwave measurements; microstrip ring resonator*

1. INTRODUCTION

Several measurement techniques have been developed for dielectric property characterization at microwave frequencies [1]. In general, resonant cavity methods provide the most accurate dielectric data; however, they are limited to single-frequency characterization. For materials with a relatively high dielectric constant, for example, 10 and above, the shift of the loaded cavity resonance frequency is found to be relatively independent of the value of the permittivity of the loading material. To overcome this limitation and to obtain accurate measurement data on microwave materials, the use of microstrip ring resonators has been proposed for material property characterization [2]. This approach is based on the relationship between the experimentally measured resonance frequencies and the effective dielectric constant. The dielectric constant of the material is determined from the value of the effective dielectric constant by using approximate closed-form expressions, such as ones give by Wheeler [3] and Hammerstad [4]. However, these closed-form formulas, derived under the quasi-TEM approximation, have limited validity, and are not sufficiently accurate when the frequency and/or the dielectric constant are high.

In a previous work [5, 6], the authors have demonstrated the feasibility of determining the dielectric constant of the substrate at high frequencies by fitting the scattering parameter spectra of microstrip ring resonators, simulated by using the FDTD method, to the experimental data. Simulations were performed for microstrip resonators with an alumina

Contract grant sponsor: Center for Dielectric Studies, Pennsylvania State University

substrate ($K \sim 9$). In this paper, we present an extension of the above ring resonator approach for high-K substrates ($K \sim 100$), and also compare the effectiveness of the method for both low- and high-K dielectrics.

2. SAMPLES AND MEASUREMENTS

Ring resonators edge coupled to the feedlines (Fig. 1) were fabricated on alumina and rutile substrates by using a standard thick-film process. The microstrip pattern was created by screen printing conducting ink onto the substrate, and the assembly was subsequently heat treated at 850°C. The dimensions of the silver conducting ring and the feedline strips were 0.25 mm wide and 0.01 mm thick, the outside diameter of the ring was 10 mm, the coupling gaps were 0.125 mm wide, and the thickness of the alumina and rutile substrates was 0.625 mm and 1.5 mm, respectively.

The scattering parameter S_{21} was measured as a function of frequency from 45 MHz to 26 GHz by using a HP8510C network analyzer. Spurious microwave reflections, occurring at the interface between the coaxial line and the microstrip, were accounted for by employing a standard two-port calibration procedure.

The microwave dielectric data were independently confirmed from a cavity technique. Before the ground plane and ring metallization were applied, the dielectric constant of the substrate was measured in a TE_{011}-mode cylindrical cavity [7].

3. SIMULATION PROCEDURE

The conformal FDTD technique [8], which allows one to model curved perfectly conducting surfaces without employing a staircasing approximation, was used for our simulations. Either Mur's absorbing boundary condition (ABC) [9] or the perfectly matched layer (PML) type of mesh truncation [10] was applied at all boundaries of the computational domain, except that a perfect electric conductor (PEC) ground plane was inserted at the bottom of the substrate. A Gauss-sine type of electric field source with a bandwidth of 10 GHz modulated by a sinusoidal wave of 5 GHz was applied between the microstrip feedline and the ground plane to excite the ring resonator.

The S_{21}-parameter was computed from the ratio of the transmitted to incident voltage, i.e., by using $S_{21} = V_{tr}(f)/V_{inc}(f)$, where $V_{inc}(f)$ and $V_{tr}(f)$ are the Fourier components of the incident and transmitted voltages at frequency f, respectively.

The transient response of a ring resonator typically exhibits a ringing behavior that lingers over a long period of time [5]. In order to accurately simulate scattering parameters in the frequency domain via the Fourier transform, it is necessary to compute the temporal response of the resonator over tens of thousands of time steps because the accuracy of the simulated scattering parameters would be compromised if the transient time record were terminated prematurely. In the FDTD simulations of ring resonators with alumina substrates [5, 6], we have used Mur's ABC, and it was found that the simulation results converged after about 16,000 time steps [5]. However, for resonators with the rutile substrate, 16,000 time steps are insufficient to accurately determine the scattering parameter spectrum. On the other hand, it was not possible to increase the number of time steps because of error accumulation introduced by the imperfect ABC. This is demonstrated in Figure 2(a), which shows the time signature of the current in the output feedline of the ring resonator with rutile substrate, simulated by using Mur's ABC. Figure 2(b) shows the corresponding result for the same problem, but simulated by using the PML boundaries for mesh truncation. Since the reflection errors are essentially negligible when the PML boundary condition is used, we are able to compute the results for many more time steps than are required for the transients to fully decay.

In order to visualize the wave propagation in microstrip lines with low- and high-K substrates, we have simulated the electromagnetic field distribution patterns for both alumina and rutile substrates.

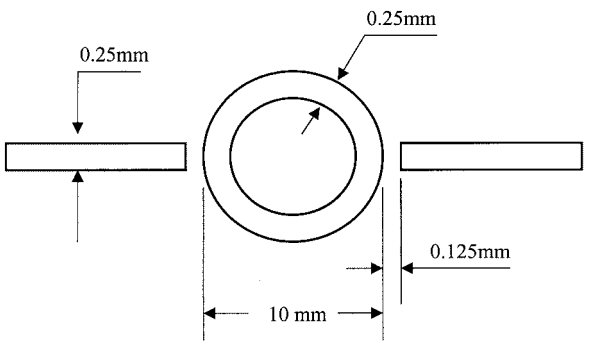

Figure 1 Ring resonator geometry

4. RESULTS

Figures 3(a) and 4(a) plot the distributions of the electric-field component normal to the substrate surface, and Figures 3(b)

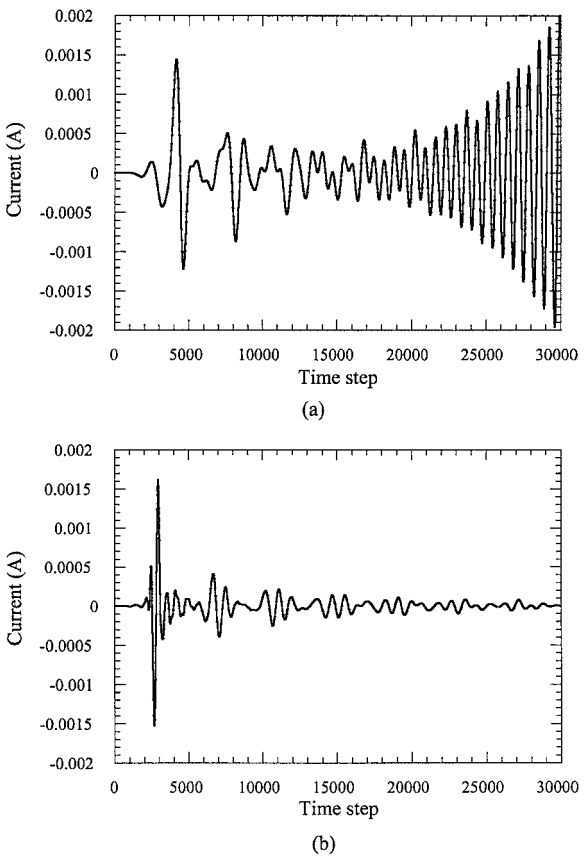

Figure 2 Transient current response in the output feedline of the ring resonator simulated using: (a) Mur's ABCs, and (b) the PML boundary conditions, respectively. The time step is equal to 0.25 ps

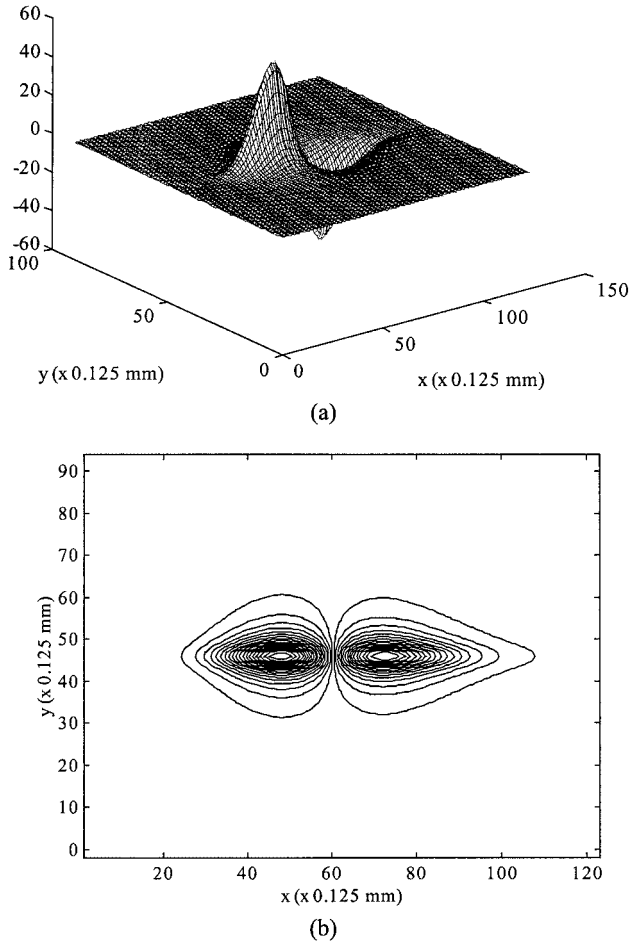

Figure 3 (a) Distribution of the electric-field component normal to the substrate surface. (b) Its contour plot at 5000 time steps in the plane located 0.3 mm beneath the microstrip in the microstrip line with alumina substrate. The time step is equal to 0.25 ps

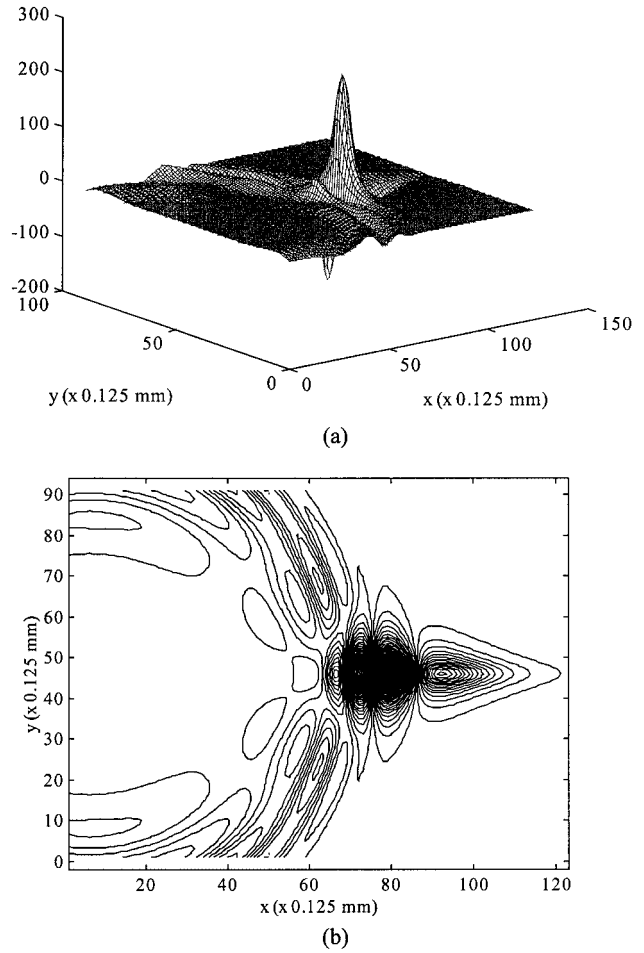

Figure 4 (a) Distribution of the electric-field component normal to the substrate surface. (b) Its contour plot at 1400 time steps in the plane located 0.3 mm beneath the microstrip in the microstrip line with rutile substrate. The time step is equal to 0.25 ps

and 4(b) are the corresponding contour plots in the plane located beneath the microstrips inside the alumina (Fig. 3) and rutile (Fig. 4) substrates. The effects of dispersion and the substrate wave propagation, accompanying the propagation of the signal, are clearly observed in the picture for the case of high-K substrate. To the best of our knowledge, the visualization of the substrate surface waves has not been previously reported in the literature. It is obvious from our results that the TEM approach cannot adequately describe the wave propagation process in high-K dielectric substrates.

Figure 5 shows the $|S_{21}|$ spectra of ring resonators with rutile substrate, simulated by using different values of the dielectric constant for the substrate. As seen from the figure, the $|S_{21}|$ spectrum is more sensitive to the permittivity value change at higher frequencies. The $|S_{21}|$ spectrum shift can be reliably resolved when the dielectric constant value changes by 1% of its initial value. In other words, the proposed method is accurate to within 1%.

Figure 6(a),(b) shows a comparison of experimentally measured $|S_{21}|$ spectra with the simulated spectra for both substrates. For the alumina substrate, the best fitting of the whole spectra was achieved when the dielectric constant of the substrate was set to equal 9.3 (± 0.1) [Fig. 5(a)]. For the rutile substrate, the best fitting dielectric constant value was 95 (± 1) [Fig. 5(b)].

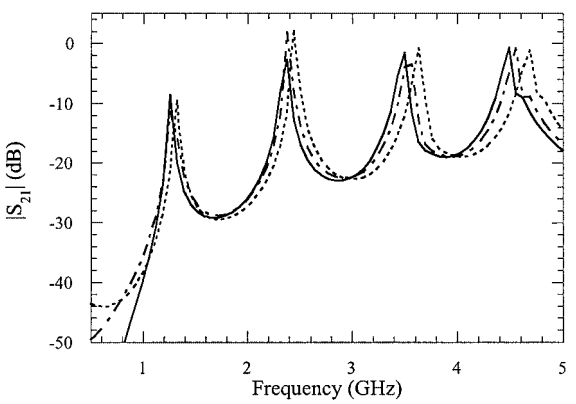

Figure 5 $|S_{21}|$ spectra simulated for a ring resonator with rutile substrate using the following dielectric constant values: $K = 90$ (dotted curve), $K = 95$ (dotted–dashed curve), and $K = 98$ (solid curve)

Figure 7 presents the dielectric constant values determined by the Wheeler–Hammerstad formula from the measured $|S_{21}|$ spectra at different resonance frequencies in comparison with the dielectric constant values obtained from FDTD simulations for both (a) alumina and (b) rutile substrates. The results of independent measurements by the

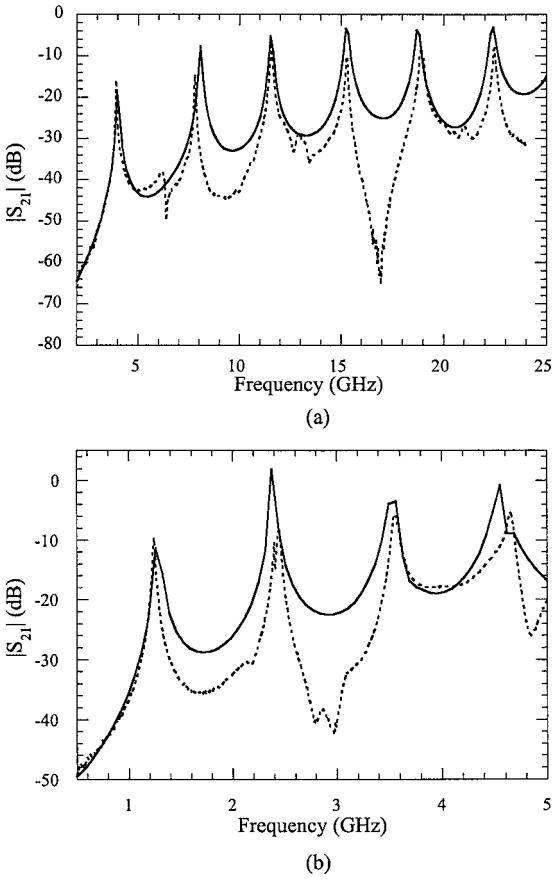

Figure 6 Experimentally measured $|S_{21}|$ spectra (dashed curves) and simulated $|S_{21}|$ spectra (solid curves) for ring resonators with: (a) alumina substrate with a dielectric constant of 9.3, and (b) rutile substrate with a dielectric constant of 95

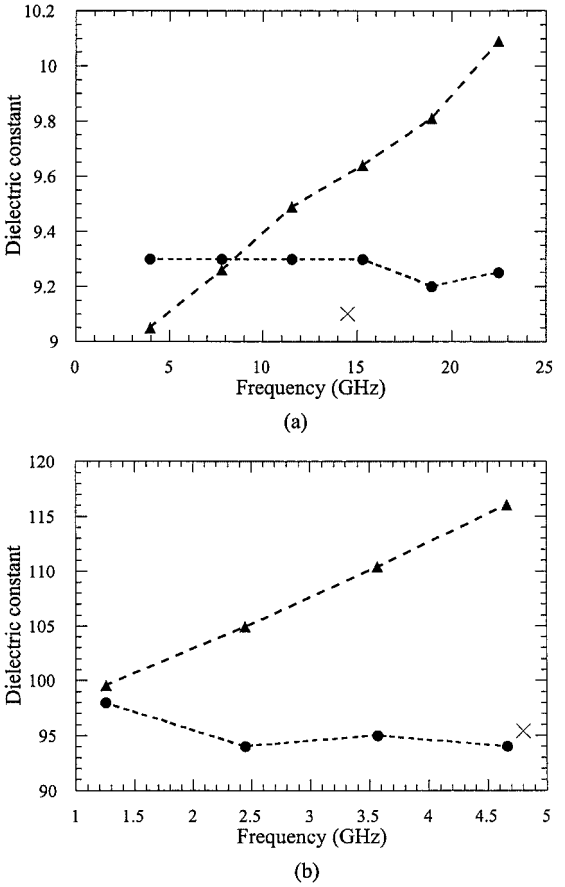

Figure 7 Dielectric constant versus frequency determined by the Wheeler–Hammerstad formula (triangles), using the FDTD simulations (circles), and cavity measurements ("×" marks) for: (a) alumina, and (b) rutile substrates, respectively

cavity technique at a frequency of 14.5 GHz for alumina substrate and at 4.8 GHz for rutile substrate are shown in Figure 7 as "×" marks. As seen from the figures, the dielectric constant value determined by the Wheeler–Hammerstad formula shows a significant increase with frequency, which is nonphysical. This result demonstrates the systematic error introduced in the dielectric constant determination by the Wheeler–Hammerstad method. In comparison with the Wheeler–Hammerstad method, our method provides results that are much more consistent with the results obtained by the cavity resonance technique.

In conclusion, we have successfully applied the FDTD method to simulate *S*-parameter spectra in microstrip ring resonators, and have accurately determined the dielectric constant of alumina and rutile substrates at microwave frequencies by fitting the simulation results to the experimental data. This method can be especially valuable for the characterization of high-*K* dielectric substrates at microwave frequencies.

ACKNOWLEDGMENT

The authors would like to thank Amanda Baker for the sample fabrication and Steve Perini for the device measurement.

REFERENCES

1. J. Baker-Jarvis and C.A. Jones, Dielectric measurements on printed-wiring and circuit boards, thin films, and substrates: An overview, Mater Res Soc Symp Proc, 1995, vol. 381, pp. 153–163.
2. P.A. Bernard and J.M. Gautray, Measurement of dielectric constant using a microstrip ring resonator, IEEE Trans Microwave Theory Tech 39 (1991), 592–595.
3. H.A. Wheeler, Transmission line properties of parallel strips separated by a dielectric shield, IEEE Trans Microwave Theory Tech MTT-13 (1965), 172–185.
4. E.O. Hammerstad, Equations for microstrip circuit design, Proc European Microwave Conf, Hamburg, Germany, Sept. 1975, pp. 268–272.
5. E. Semouchkina, W. Cao, and R. Mittra, Modeling of microwave ring resonators using the finite-difference time-domain (FDTD) method, Microwave Opt Technol Lett 24 (2000), 392–396.
6. E. Semouchkina, W. Cao, and M. Lanagan, High frequency permittivity determination by spectra simulation and measurement of microstrip ring resonators, Electron Lett 36 (2000), 956–958.
7. G. Kent, Nondestructive permittivity measurement of substrates, IEEE Trans Instrum Meas 45 (1996), 102–106.
8. W. Yu and R. Mittra, Accurate modeling of planar microwave circuit using conformal FDTD algorithm, Electron Lett 36 (2000), 618–619.
9. G. Mur, Absorbing boundary conditions for the finite-difference approximation of the time-domain electromagnetic-field equations, IEEE Trans Electromag Compat EMC-23 (1981), 377–382.
10. S.D. Gedney, An anisotropic perfectly matched layer-absorbing medium for the truncation of FDTD lattices, IEEE Trans Microwave Theory Tech 44 (1996), 1630–1639.